

Semiclassical Double-Pomeron Production of Glueballs and η'

Edward Shuryak and Ismail Zahed

Department of Physics and Astronomy, State University of New York, Stony Brook, NY 11794

(November 8, 2018)

A semiclassical theory of high energy scattering based on interrupted tunneling (instantons) or QCD sphaleron production has been recently developed to describe the growing hadronic cross section and properties of the soft Pomeron. In this work we address double-pomeron processes in this framework for the first time. We specifically derive the cross section for central production of parity even and odd clusters, scalar and pseudoscalar glueballs, and η' in parton-parton scattering at high energy. We show that the specific dependence of the production cross section on all its kinematical variables compares favorably with the UA8 data on inclusive cluster production, as well as the WA102 data on exclusive central production of scalar glueball and η' , in double-pomeron exchange pp scattering. The magnitude of the cross section and its dependence on kinematic variables is correct, explaining in particular a large deviation from the Pomeron factorization at cluster masses in the range $M_X < 8$ GeV reported by UA8.

I. INTRODUCTION

Semi-classical tunneling in the QCD vacuum, described by instantons, is traditionally studied in relation with the QCD vacuum properties such as chiral symmetry breaking and hadronic spectroscopy, see review [1].

More recently a number of authors [2,3] have suggested that the semiclassical physics based on instantons and QCD sphalerons significantly contributes to semi-hard scattering in QCD, in particular to the parameters of the so called “soft Pomeron”. The specific behavior of hadronic cross sections at high energy, i.e. their growth with energy $\sigma \sim s^{0.08}$ is related to the Pomeron trajectory intercept at $t = 0$. The semiclassical theory relates the small power of 0.08 to the barrier-suppressed probability of tunneling in the QCD vacuum. Also, the small Pomeron size $\alpha' = 1/(2 \text{ GeV})^2 = (0.1 \text{ fm})^2$ was found to be related in [2,3] to the small instanton size $\rho = 1/3 \text{ fm}$. As unexpected bonus, it was found that the semiclassical scattering cannot produce an *odderon*, essentially due to the inherent $SU(2)$ color nature of the semiclassical fields. Recently, the same semiclassical reasoning was applied to the saturation problem at HERA [4].

The semiclassical approach to semi-hard processes is distinct from many QCD models in a number of ways. It describes field excitations from the under-the-barrier part of vacuum wave function, becoming on-the-barrier states referred to as QCD sphalerons. They are specific topological clusters made of purely magnetic glue [5]. As quantum-mechanical and semi-classical arguments show, it is the most natural excitation of the glue from under the barrier. When produced they explode [5,6], creating on the way many light quark pairs [7].

The corresponding contributions to the soft Pomeron can be viewed as a ladder-type diagrams, similar to the perturbative BFKL ones but with different rungs [3,2]. The Lipatov vertex – 2 virtual gluons fusing into one physical gluon – is substituted by a new vertex with a tunneling path ending at the unitarity cut at the “turning state” -the topological clusters. In this work we focus on only one cluster production as illustrated in Fig. 1.

In contrast to deep-inelastic scattering, high energy hadronic collisions in the semi-hard regime have no large scale Q^2 , and so the produced clusters have masses and sizes that are determined by the typical size of the instantons in the QCD vacuum. This leads to a mass of order 3 GeV for a size of order 1/3 fm, as mentioned above.

A significant amount of clustering in pp collisions has been known for a very long time [8], where it was also pointed out that those clusters have on average larger mass and multiplicity in comparison to the clusters produced in e^+e^- annihilation. Unfortunately, a study of these clusters and their identification is still not done. In general, from the analysis of secondaries in pp collisions it is hard to tell which clusters are sphaleron-related and produced promptly, and which are simply products of the string fragmentation, a final state interaction unrelated to the underlying dynamics responsible for the cross section. In ordinary inclusive pp collisions only a bulk statistical analysis can be performed.

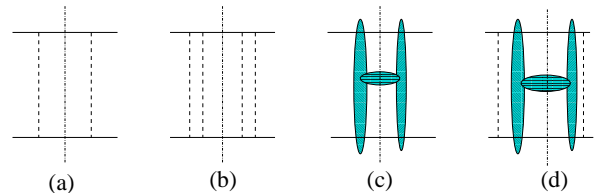


FIG. 1. Schematic diagrams for the cross sections of different processes associated with high energy collision of two quarks, shown by horizontal solid lines. The vertical dash-dotted lines are unitarity cuts, they separate the amplitude from its complex conjugate. (a) Low-Nussinov or single-gluon exchange, leading to inelastic collisions due to color exchange; (b) Low-Nussinov cross section, with no color exchange; (c) instanton-induced inelastic collision with color transfer and prompt cluster production, (d) combined instanton-gluon process leading to double-pomeron like events with a cluster.

That is why in the present work we focus on double-pomeron scattering, or processes in which there are two

large *rapidity gaps* separating the colliding two protons with a single cluster produced at mid-rapidity. In this case there is no place for color strings and their fragmentation, as all object involved are colorless. So, if our assumption about dominance of the topological clusters is correct, we should be able to describe the double-pomeron data solely from the semiclassical theory. The answer is yes, as we will detail below.

Important experimental findings on *inclusive* double diffraction were recently reported by the UA8 collaboration [9], based on its 1989 data data sample at CERN $S\bar{p}pS$ collider. We note in this work that the reported data display a wide maximum around cluster masses of order few GeV, with a cross section that is an order of magnitude larger than the one predicted by Pomeron factorization. Interestingly enough, the clusters with mass less than 5 GeV decay isotropically in their rest frame. Unfortunately, the UA2 detector used in this work was a simple calorimeter with poor mass resolution with sigma about 2 GeV, which prohibited from seeing mass structure in our pomeron-pomeron cross section.

The WA102 collaboration at CERN carried a fixed target pp experiment at $\sqrt{s} = 28$ GeV, focusing on the double-pomeron exclusive production into few hadron states. This experiment was the first to discover a strong dependence of the cross section on the azimuthal angle between the momenta transferred to two protons, a feature that was not expected from standard Pomeron phenomenology. This result inspired some phenomenological works [10–12] pointing a possible analogy between the Pomeron and vector particles. Close and his collaborators have even suggested to use this azimuthal distribution as a glueball filter, selecting the hadronic states which peak at small difference in transverse momentum dP_T of the protons. In particular, the production of scalars and tensors such as $f_0(980)$, $f_0(1500)$, $f_J(1710)$, and $f_2(1900)$ was found to be considerably enhanced at small dP_T , while the production of pseudoscalars such as η , η' was found to be peaked at mutually orthogonal momentum transfers of the protons. In our approach the produced QCD sphalerons can be regarded as precursors of glueballs or pseudoscalar η' strongly coupled to glue. In the double-pomeron process the sphaleron production dwarfs the instanton-antiinstanton process [12] by 2 orders of magnitude, and contrary to the latter it triggers a rise in the cross section.

The paper is organized as follows: In section 2 we recall the general expression for the total QCD cross section in the eikonal approximation, and check its perturbative (Low-Nussinov) limit. In section 3 we analyze the generic form of the double-pomeron cross section and show its direct relationship with the inelastic cross section through the Pomeron. In section 4, we discuss the double-pomeron inclusive UA8 results in light of our results. In section 5, we derive explicit results for the even/odd double-pomeron gluon production. In section 6 we use the scale and U(1) anomaly to derive the double-pomeron cross sections for isosinglet produc-

tion. In section 7, we compare our results to the CERN WA102 results for the reported glueball and η' states. Our conclusions are in section 8.

II. TOTAL CROSS SECTION

In this section and to help streamline the definitions, we quote the general result for the instanton-induced contribution to the total cross section, and check its perturbative limit.

A. General Result

The generic form of the total cross section for parton-parton scattering through a generic gauge configuration in QCD reads at large \sqrt{s} [2]

$$\begin{aligned} \sigma &\approx \frac{\text{Im}}{VT} \sum_{CD} \frac{1}{(2\pi)^6} \int dq_{1+} dq_{1\perp} dq_{2-} dq_{2\perp} \\ &\times \int [dA][dA'] e^{iS(A)-iS(A')+iS(A,A')} \\ &\times \int dx_- dx_\perp dy_+ dy_\perp e^{\frac{i}{2}q_{1+}x_- - iq_{1\perp}x_\perp + \frac{i}{2}q_{2-}y_+ - iq_{2\perp}y_\perp} \\ &\times (\mathbf{W}_-(\infty, x_-, x_\perp) - \mathbf{1})_{AC} (\mathbf{W}_+(y_+, \infty, y_\perp) - \mathbf{1})_{BD} \\ &\times \int dx'_- dx'_\perp dy'_+ dy'_\perp e^{\frac{i}{2}q_{1+}x'_- - iq_{1\perp}x'_\perp + \frac{i}{2}q_{2-}y'_+ - iq_{2\perp}y'_\perp} \\ &\times (\mathbf{W}_-(\infty, x'_-, x'_\perp) - \mathbf{1})_{AC}^* (\mathbf{W}_+(y'_+, \infty, y'_\perp) - \mathbf{1})_{BD}^* . \end{aligned} \quad (1)$$

which is the imaginary part of a retarded 4-point correlation function in Minkowski space. The line integrals are along the light cone with

$$\begin{aligned} \mathbf{W}_-(\infty, x_-, x_\perp) &= \\ \mathbf{P}_c \exp \left(-\frac{ig}{2} \int_{-\infty}^{+\infty} dx'_+ A_-(x'_+, x_-, x_\perp) \right) . \end{aligned} \quad (2)$$

and

$$\begin{aligned} \mathbf{W}_+(x_{1+}, \infty, x_\perp) &= \\ \mathbf{P}_c \exp \left(-\frac{ig}{2} \int_{-\infty}^{+\infty} dx'_- A_+(x_+, x'_-, x_\perp) \right) . \end{aligned} \quad (3)$$

B. Low-Nussinov Limit

In perturbation theory, the line integrals can be expanded to give in the lowest perturbative order

$$\mathbf{W}_+ - \mathbf{1} \approx -\frac{ig}{2} \int_{-\infty}^{+\infty} dx'_- A_+(x_+, x'_-, x_\perp) \quad (4)$$

and similarly for \mathbf{W}_- . The correlator of two vector potentials is the gluon propagator, so the expression corresponds to a diagram shown in Fig.1(a). Inserting (4) into (1) we obtain to leading order in perturbation theory

$$\sigma \approx \left(\frac{\alpha_s}{\pi}\right)^2 \left(\frac{T^e T^f}{2 \ 2}\right)_{AA} \left(\frac{T^e T^f}{2 \ 2}\right)_{BB} \int \frac{dq_\perp}{\pi^2} \times \left| \int db_\perp e^{-iq_\perp b_\perp} \int d\alpha d\beta \frac{v_+ \cdot v_-}{(v_+ \alpha - v_- \beta)^2 - b_\perp^2 + i0} \right|^2 \quad (5)$$

where v_\pm are the 4-velocities on the light-cone with proper-time extent T . The result (5) is

$$\sigma \approx \left(\frac{4\alpha_s}{\pi}\right)^2 \left(1 - \frac{1}{N_c^2}\right) \times \int dq_\perp \left| \int db_\perp e^{-iq_\perp b_\perp} \ln\left(\frac{T}{b_\perp}\right) \right|^2, \quad (6)$$

after proper color tracing, in agreement with the perturbative result of Low-Nussinov [13].

III. DOUBLE-POMERON CROSS SECTION

The exclusive cross section for the double-pomeron parton-parton scattering $qq \rightarrow qqX$ where X stands for a centrally produced color singlet cluster as diagrammatically depicted in Fig. 1 (d). The vertical ellipses indicate instantons and the dashed line is an additional perturbative gluon that is needed to enforce overall color neutrality for the state X emitted in the central region. The thin vertical lines in all diagrams denotes the unitarity cut. The corresponding exclusive cross section reads

$$\begin{aligned} \sigma &\approx \frac{\text{Im}}{VT} \frac{1}{(2\pi)^6} \int dq_{1+} dq_{1\perp} dq_{2-} dq_{2\perp} \\ &\times \int [dA][dA'] e^{iS(A) - iS(A') + iS(A,A')} \\ &\times \int dx_- dx_\perp dy_+ dy_\perp e^{\frac{i}{2}q_{1+}x_- - iq_{1\perp}x_\perp + \frac{i}{2}q_{2-}y_+ - iq_{2\perp}y_\perp} \\ &\times \left(\frac{-ig}{2} \int_{-\infty}^{+\infty} dz_+ A_-(z_+, x_-, x_\perp) \mathbf{W}_-(\infty, x_-, x_\perp)\right)_{AA} \\ &\times \left(\frac{-ig}{2} \int_{-\infty}^{+\infty} dz_- A_-(y_+, z_-, y_\perp) \mathbf{W}_+(y_+, \infty, y_\perp)\right)_{BB} \\ &\times \int dx'_- dx'_\perp dy'_+ dy'_\perp e^{\frac{i}{2}q_{1+}x'_- - iq_{1\perp}x'_\perp + \frac{i}{2}q_{2-}y'_+ - iq_{2\perp}y'_\perp} \\ &\times \left(\frac{-ig}{2} \int_{-\infty}^{+\infty} dz'_+ A'_-(z'_+, x'_-, x'_\perp) \mathbf{W}_-(\infty, x'_-, x'_\perp)\right)_{AA}^* \\ &\times \left(\frac{-ig}{2} \int_{-\infty}^{+\infty} dz'_- A'_-(y'_+, z'_-, y'_\perp) \mathbf{W}_+(y'_+, \infty, y'_\perp)\right)_{BB}^*. \end{aligned} \quad (7)$$

The leading order contribution to (7) stems from the perturbative part of the gluon exchanged in Fig. 1 around the semiclassical background attached to the eikonal partons. The former increases with the proper-length of the eikonalized trajectories spanned by the incoming partons. The result is

$$\begin{aligned} \sigma &\approx \frac{\text{Im}}{VT} \frac{1}{(2\pi)^6} \int dq_{1+} dq_{1\perp} dq_{2-} dq_{2\perp} \\ &\times \int [dA][dA'] e^{iS(A) - iS(A') + iS(A,A')} \\ &\times \int dx_- dx_\perp dy_+ dy_\perp e^{\frac{i}{2}q_{1+}x_- - iq_{1\perp}x_\perp + \frac{i}{2}q_{2-}y_+ - iq_{2\perp}y_\perp} \\ &\times 2\alpha_s \ln\left(\frac{T}{|x_\perp - y_\perp|}\right) \\ &\times \left(\frac{T^a}{2} \mathbf{W}_-(\infty, x_-, x_\perp)\right)_{AA} \left(\frac{T^a}{2} \mathbf{W}_+(y_+, \infty, y_\perp)\right)_{BB} \\ &\times \int dx'_- dx'_\perp dy'_+ dy'_\perp e^{\frac{i}{2}q_{1+}x'_- - iq_{1\perp}x'_\perp + \frac{i}{2}q_{2-}y'_+ - iq_{2\perp}y'_\perp} \\ &\times 2\alpha_s \ln\left(\frac{T}{|x'_\perp - y'_\perp|}\right) \\ &\times \left(\frac{T^b}{2} \mathbf{W}_-(\infty, x'_-, x'_\perp)\right)_{AA}^* \left(\frac{T^b}{2} \mathbf{W}_+(y'_+, \infty, y'_\perp)\right)_{BB}^*. \end{aligned} \quad (8)$$

The non-perturbative parts of the gluon propagator in Feynman background gauge have been dropped. The perturbative part dominates through its logarithmic growth at large proper time T .

A. Details

The result (8) is general and holds in Minkowski space. Following our previous arguments we assess the imaginary part by continuing to Euclidean space and saturating the double functional integral with singular gauge configurations which are sphaleron-like. The result can be considerably simplified if we note that the 2-dimensional Coulombic law probes transverse distances $|x_\perp - y_\perp|$ of the order of the sphaleron size ρ , while the Euclidean time T is of the order of the inverse sphaleron mass $1/M_s$. As a result and modulo color factors, the 2-dimensional Coulomb contribution brings about an overall factor of

$$4\alpha_s^2 \ln^2(\rho M_s) = 4\alpha_s^2 \ln^2\left(\frac{4\alpha_s}{3\pi}\right). \quad (9)$$

The color factors can be unwound by using

$$\mathbf{W} = \cos \alpha - i \mathbf{R}^{ai} \tau^a \mathbf{n}^i \sin \alpha \quad (10)$$

where the singular gauge configuration is given by α ¹. Specifically, the contribution

$$\begin{aligned}
& -i\mathbf{R}^{ai}\mathbf{n}^i \left(\frac{T^e}{2}\tau^a\right)_{AA} \sin\alpha \\
& \times -i\mathbf{R}^{bj}\mathbf{n}^j \left(\frac{T^e}{2}\tau^b\right)_{BB} \sin\alpha \\
& \times +i\mathbf{R}^{a'i'}\mathbf{n}^{i'} \left(\frac{T^f}{2}\tau^{a'}\right)_{AA}^* \sin\alpha' \\
& \times +i\mathbf{R}^{b'j'}\mathbf{n}^{j'} \left(\frac{T^f}{2}\tau^{b'}\right)_{BB}^* \sin\alpha'
\end{aligned} \quad (11)$$

where the T^e 's are $SU(N_c)$ generators with $e = 1, \dots, (N_c^2 - 1)$ and τ^a 's are $SU(2)$ generators with $a = 1, 2, 3$, can be simplified using the color averaging relation

$$\left(\frac{T^e}{2}\tau^a\right)_{AA} \equiv \frac{1}{N_c} \text{Tr} \left(\frac{T^e}{2}\tau^a\right) = \frac{\mathbf{1}^{ea}}{N_c}. \quad (12)$$

Thus, (11) becomes

$$\frac{1}{N_c^4} \mathbf{n} \cdot \mathbf{n} \mathbf{n}' \cdot \mathbf{n}' \sin\alpha \sin\alpha' \sin\alpha' \quad (13)$$

B. Inclusive Double-Pomeron Cross Section

Inserting (9-13) into (8) and following the steps given in [2], we obtain for the total singlet cross section

$$\begin{aligned}
\sigma(s) & \approx \mathbf{C}_S \pi \rho^2 \ln s \int dq_{1\perp} dq_{2\perp} \mathbf{K}(q_{1\perp}, q_{2\perp}) \\
& \times \int_{(q_{1\perp}+q_{2\perp})^2}^{\infty} dM^2 \sigma_S(M). \quad (14)
\end{aligned}$$

The constant \mathbf{C}_S is equal to

$$\mathbf{C}_S = \frac{1}{(2\pi)^8} \frac{64}{5N_c^2} \alpha_s^2 \ln^2 \left(\frac{4\alpha_s}{3\pi}\right). \quad (15)$$

The partial cross section $\sigma_S(Q)$ is the same as the one encountered in the sphaleron-like production. To exponential accuracy

$$\sigma_S(Q) = \text{Im} \int dT e^{QT - \mathbf{S}(T)} \approx \kappa e^{\frac{4\pi}{\alpha} (\mathbf{F}(Q) - \mathbf{F}(M_s))}, \quad (16)$$

where the holy grail function $\mathbf{F}(Q)$ was evaluated in [14,6] using singular gauge configurations. In the approximation

$$\sigma_S(Q) \approx \kappa \delta(Q^2 - M_s^2) \quad (17)$$

the singlet cross section simplifies to

$$\sigma(s) \approx \mathbf{C}_S \pi \rho^2 \kappa \ln s \int dq_{1\perp} dq_{2\perp} \mathbf{K}(q_{1\perp}, q_{2\perp}), \quad (18)$$

which is analogous to the inelastic (Pomeron induced) cross section derived in [2] with the substitution $\mathbf{C}_S \rightarrow \mathbf{C}$ where

$$\mathbf{C} = \frac{1}{(2\pi)^8} \frac{64}{15} \quad (19)$$

Note that the ratio of the semiclassical double-pomeron cross section to the semiclassical inelastic cross section, as given by diagrams Fig. 1d and 1c respectively, is independent of the detailed dynamics, and involves mostly color factors resulting from the singlet projection through the extra gluon exchanged

$$\frac{\sigma_{DD}}{\sigma_{IN}} \approx \frac{\mathbf{C}_S}{\mathbf{C}} = \frac{3}{N_c^2} \alpha_s^2 \ln^2 \left(\frac{4\alpha_s}{3\pi}\right) \approx 0.125. \quad (20)$$

C. The instanton-induced form factor

The form factor is

$$\mathbf{K}(q_{1\perp}, q_{2\perp}) = |\mathbf{J}(q_{1\perp}) \cdot \mathbf{J}(q_{2\perp}) + \mathbf{J}(q_{1\perp}) \times \mathbf{J}(q_{2\perp})|^2, \quad (21)$$

with

$$\mathbf{J}(q_{\perp}) = \int dx_3 dx_{\perp} e^{-iq_{\perp}x} \frac{x_{\perp}}{|x|} \sin \left(\frac{\pi|x|}{\sqrt{x^2 + \rho_0^2}}\right). \quad (22)$$

which is purely imaginary,

$$\begin{aligned}
\mathbf{J}(q_{\perp}) & = -i \frac{\hat{q}_{\perp}}{\sqrt{q_{\perp}}} \int_0^{\infty} dx J_{3/2}(q_{\perp}x) \\
& \times \left((2\pi x)^{3/2} \sin \left(\frac{\pi|x|}{\sqrt{x^2 + \rho_0^2}}\right) \right). \quad (23)
\end{aligned}$$

Here $J_{3/2}$ is a half-integer Bessel function. In the weak-field limit the instanton contributes a term $3\sqrt{x}/x^2 \approx 1/\sqrt{x}$ that causes the instanton-induced form factor to diverge. This divergence is analogous to the one encountered in $QQ \rightarrow QQ$. Apart from the unphysical (perturbative) singularity at small q_{\perp} , the instanton-induced form factor can be parameterized by a simple exponential

$$\mathbf{J}(q_{\perp}) \approx -i \hat{q}_{\perp} 50 e^{-1.3q_{\perp}\rho_0}, \quad (24)$$

The divergence at small q_{\perp} can be removed by subtracting the tail of the instanton through the substitution

$$\frac{\pi|x|}{\sqrt{x^2 + \rho_0^2}} \rightarrow \pi \left(\frac{|x|}{\sqrt{x^2 + \rho_0^2}} - 1 \right) e^{-\mathbf{a}|x|/\rho_0}, \quad (25)$$

which amounts to a different renormalization of the charge. This will be understood throughout. Note that the subtracted form factor vanishes at small q_{\perp} .

¹Since the singular gauge configuration asymptotes the instanton profile, it is sufficient to use the instanton/antiinstanton profile in the form factors.

IV. INCLUSIVE DOUBLE-POMERON: UA8

The UA8 experiment at CERN studied the reaction $\bar{p}p \rightarrow \bar{p}Xp$ where X is a set of hadrons at mid-rapidity. There are two sets of data: one in which both nucleons were detected (AND) and one in which only one nucleon was detected (OR). Since the two triggers are different, the two data sets were measured at different kinematics. UA8 used the following model-dependent parametrization of their measured differential cross section

$$\frac{d^6\sigma_{DPE}}{d\xi_1 d\xi_2 dt_1 dt_2 d\phi_1 d\phi_2} = F_{\mathcal{P}/p}(t_1, \xi_1) \cdot F_{\mathcal{P}/p}(t_2, \xi_2) \cdot \sigma_{\mathcal{P}\mathcal{P}}^{tot}(M_X). \quad (26)$$

where the variables (ξ_i, t_i, ϕ_i) describe the fraction of the longitudinal momentum, momentum transfer squared and its azimuthal direction for each Pomeron. All the parameters are uniquely given by the measured parameters of the outgoing p, \bar{p} . The Pomeron flux factor or structure function is defined as

$$F_{\mathcal{P}/p}(t, \xi) = K |\mathbf{F}_1(t)|^2 e^{bt} \xi^{1-2\alpha(t)} \quad (27)$$

where $|\mathbf{F}_1(t)|^2$ is the so called Donnachie-Landshoff [15] nucleon form factor

$$\mathbf{F}_1(t) = \frac{4m_p^2 - 2.8t}{4m_p^2 - t} \frac{1}{(1 - t/0.71)^2}. \quad (28)$$

The parameters were defined from single-pomeron data with $b = 1.08 \pm 0.2 \text{ GeV}^{-2}$, and nonlinear Pomeron trajectory

$$\begin{aligned} \alpha(t) &= 1 + \epsilon + \alpha't + \alpha''t^2 \\ &= 1.035 + 0.165t + 0.059t^2. \end{aligned} \quad (29)$$

The parameter $K = 0.74/\text{GeV}^2$ was not measured and was set from the Donnachie-Landshoff fit. The specific parametrizations (??-traj) were used to set up the acceptances and so on. However, in the UA8 paper to be discussed below, it was pointed out that the difference between the AND and OR data sets may suggest that the above parametrization with factorizable flux factors maybe oversimplified.

The uncertainties related to the empirical extrapolation from the covered to the full kinematical range notwithstanding, the UA8 data show a striking and an unexpected shape and magnitude ² for the pomeron-pomeron cross section $\sigma_{\mathcal{P}\mathcal{P}}^{tot}(M_X)$ shown in Fig. 2. Only at the central cluster mass $M_X > 10 \text{ GeV}$ was the cross section small $\approx 0.1 \text{ mb}$, and more or less in agreement with standard Pomeron calculus (more specifically with

the Pomeron factorization appended by some Reggeon contributions decreasing with M_X). At smaller masses $M_X < 10 \text{ GeV}$ the observed cross section is an order of magnitude larger than what is expected from factorization. This was neither predicted prior to the experiment, nor explained (to our knowledge) after the experiment. Another crucial finding is that the low-mass clusters decay isotropically (in their rest frame).

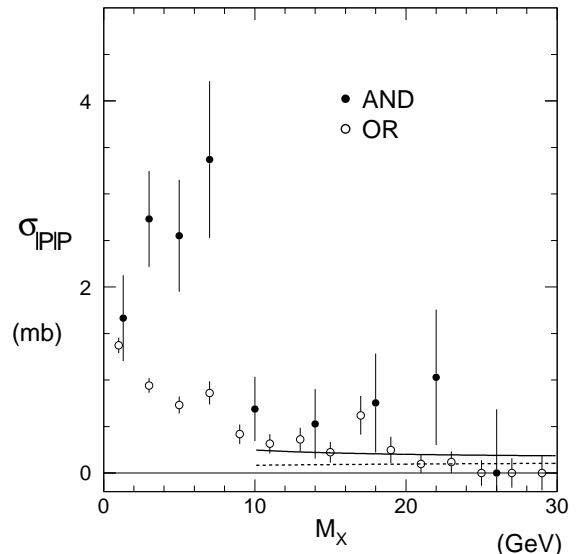


FIG. 2. Mass dependence of the Pomeron-Pomeron total cross section $\sigma_{\mathcal{P}\mathcal{P}}^{tot}$, derived from the AND and OR triggered data, respectively. The dashed curve is the factorization prediction (independent of K) for the Pomeron-exchange component of $\sigma_{\mathcal{P}\mathcal{P}}^{tot}$. The solid line is the fit to the OR points of a regge-exchange term, $1/(M_X^2)^{0.32}$, added to this Pomeron-exchange term.

Now, let us see to what extent our semiclassical description is able to describe these observations. We start with a qualitative argument of why the factorization does not work in our approach. This happens because instead of a single universal Pomeron pole we view high energy scattering in the semi-hard regime as a superposition of two different phenomena: color exchanges (which leads to a constant cross section, that does not grow with \sqrt{s}) and the topological cluster production. The single-pomeron may be caused by the former component alone, while the double-pomeron may produce a visible cluster which we will try to associate with the latter. Let us now compare the dependence of the different kinematical observables in the UA8 parameterization given above and in our semiclassical formulae.

The ϕ -dependence is explicitly³ absent in (26). The

²The extracted cross section is based on the value of K quoted above.

³Implicitly there is some dependence due to kinematical lim-

same is true in our expressions, if the total sum of the even and odd parity combinations is taken.

The t_1, t_2 -dependence factorizes in both cases. Naturally, since the UA8 expression is written for nucleons while we deal with partons, their expression has the nucleon form factor and ours does not. The remaining factor in the UA8 parameterization is

$$F_{UA8} = e^{-q^2 (b+2\alpha' \log(1/\xi))} \approx e^{-q^2 2.6 \text{GeV}^{-2}} \quad (30)$$

while we have a square of our basic form-factor $F_{our} = |\mathbf{J}(q)|^2$. Although different in shape, they are not so much different in the range $t = 1\text{-}2 \text{ GeV}^2$ in which the experiment has been done. The main scale of the object involved is obviously very close in both cases. Below we will discuss in more detail the WA102 data, which have a wider coverage on the t -dependence,

The ξ -dependence. In the first approximation, putting $\alpha(0) \approx 1$ into (26), one finds just $d\xi_1 d\xi_2 / \xi_1 \xi_2 = dy_1 dy_2$ where $y_{1,2}$ are Pomeron rapidities, giving a flat rapidity distribution of a cluster. This contributes $\ln(s)$ to the cross section. The same dependence is seen in our formulae as well. In the next approximation one has a correlation between ξ and the transverse momenta in (26), but this was most probably never really tested directly in those data, we think.

The M_X -dependence is of course the main issue. The UA8 results are shown in Fig. 2 above. Our qualitative expectations are a peak at the sphaleron mass, around 3 GeV. This is not in contradiction with the data, especially with the more kinematically constrained ‘‘AND’’ set. Unfortunately the low statistics and rather crude resolution of the UA8 experiment in M_X leaves many unanswered questions. As we have shown in [6], at this point we can only calculate the low and high- M_X parts separately, with the complete treatment in between still missing. So far we do not have a complete semiclassical prediction for the exact shape of the M_X dependence, but we are working on it.

The magnitude of the double-pomeron cross section can be estimated qualitatively. One of the reason for that is that our quark-quark cross section should be extended to qg, gg collisions and convoluted with appropriate structure functions. Those should be normalized at the semi-hard scale corresponding to $-t \sim 1\text{-}2 \text{ GeV}^2$ and the instanton size. How to do so was discussed in [16]. In short, each gluon gets an extra factor of 2 in the cross section relative to a quark (SU(2) color scaling). The total number of relevant partons was defined there as the integrated structure functions above $\xi > 0.01$, giving about $N_g \approx 4$ gluons and $N_q \approx 4$ quarks (including the sea and valence quarks), and the elementary

instanton-induced cross section for quark-quark collision $\sigma_{qq} \sim .017 \text{ mb}$. Multiplying all with the extra factor for color singletness (double-pomeron) as in (20), we estimate the total double-pomeron cross section for two nucleons to be about $\sigma_{DD}^{NN} \sim 0.2 \text{ mb}$, or about 1 percent of the Pomeron-related part of the cross section. Parametrically this smallness comes from the first power of the instanton diluteness parameter $\kappa = n\rho^4 \sim (1/3)^4$ and α_s in (20) for the extra gluon.

The experimental total double-pomeron cross section is clearly in the same ball-park, although an accurate determination by extrapolation of the UA8 data to the whole kinematical region is too uncertain to quote any specific number.

V. PARITY EVEN AND ODD CLUSTERS

The cross section (14) can easily be separated into the even/odd parity contributions following the natural parity separation in the form factor (21). The even parity combination is

$$|\mathbf{J}(q_{1\perp}) \cdot \mathbf{J}(q_{2\perp})|^2 = \cos^2 \phi |\mathbf{J}(q_{1\perp})|^2 |\mathbf{J}(q_{2\perp})|^2 \quad (31)$$

while the odd parity combination is

$$|\mathbf{J}(q_{1\perp}) \times \mathbf{J}(q_{2\perp})|^2 = \sin^2 \phi |\mathbf{J}(q_{1\perp})|^2 |\mathbf{J}(q_{2\perp})|^2 \quad (32)$$

where ϕ is the azimuthal angle between $(q_{1\perp}, q_{2\perp})$. The double-pomeron cross section for positive and negative parity glue emission are therefore (per unit rapidity η)

$$\begin{aligned} \frac{d\sigma_+}{dQ^2 dq_{1\perp} dq_{2\perp} d\eta} &= \cos^2 \phi \mathbf{C}_S \pi \rho^2 |\mathbf{J}(q_{1\perp})|^2 |\mathbf{J}(q_{2\perp})|^2 \sigma_S(Q) \\ \frac{d\sigma_-}{dQ^2 dq_{1\perp} dq_{2\perp} d\eta} &= \sin^2 \phi \mathbf{C}_S \pi \rho^2 |\mathbf{J}(q_{1\perp})|^2 |\mathbf{J}(q_{2\perp})|^2 \sigma_S(Q) . \end{aligned} \quad (33)$$

where \mathbf{C}_S can also be rewritten as

$$\mathbf{C}_S = \frac{3}{N_c^2} \alpha_s^2 \ln^2 \left(\frac{4\alpha_s}{3\pi} \right) \frac{\Delta(0)}{\kappa} \left(\int dq_{\perp} \mathbf{J}^2(q_{\perp}) \right)^{-2} \quad (34)$$

with $\Delta(0) \approx 0.1$ the ‘Pomeron’ intercept. The sum of the two, as noted before, is thus predicted to be independent of ϕ .

$$\frac{d\sigma}{dx d\phi dt_1 dt_2} / \frac{d\sigma}{dQ^2 dq_{1\perp} dq_{2\perp}} = \pi s x \quad (35)$$

for symmetric kinematics with

$$\begin{aligned} q_1 &= ((1-x_1)\sqrt{s}, -q_{1\perp}, (1-x_1)\sqrt{s}) \\ q_2 &= ((1-x_2)\sqrt{s}, -q_{2\perp}, -(1-x_2)\sqrt{s}) , \end{aligned} \quad (36)$$

$x_1 = x_2 = 1-x$, $t_1 = t_2 = t$, $|q_{1\perp}| = |q_{2\perp}| = \sqrt{-t}$, and

$$Q^2 = s x^2 + 2t(1 + \cos \phi) . \quad (37)$$

itations: not all values of the angle between \vec{q}_1, \vec{q}_2 lead to positive M_X .

VI. ISOSINGLET SCALAR AND PSEUDOSCALAR PRODUCTION

The double-pomeron cross section for even/odd parity gluon production can be readily translated to the isosinglet scalar (s_0) and pseudoscalar (η_0) $\bar{q}q$ double-pomeron cross sections through the scale and U(1) anomaly in QCD. In the instanton vacuum the induced interaction is given by [17]

$$\mathcal{S} = + \int dz \frac{1}{2\chi_*} \left(\chi(z) + i\chi_* \sqrt{2N_f} \eta_0(z) \right)^2 + \int dz \frac{1}{2\sigma_*^2} \left(\sigma(z) + i\sigma_*^2 \sqrt{2N_f} s_0(z) \right)^2, \quad (38)$$

where σ_*^2 and χ_* are the compressibility and topological susceptibility for fermionless QCD.

For small Q^2 the sphaleron induced double-pomeron cross section is mostly mediated by a singular instanton-antiinstanton configuration, which is about 1 quasiparticle before the unitarity cut. Thus the mixing (38) amounts to respectively multiplying the gluon amplitudes by

$$\frac{\sqrt{2N_f} \chi_* \rho^4}{\sqrt{2N_f} \sigma_*^2 \rho^4}, \quad (39)$$

for the odd/even parities respectively. So we get from the parity even/odd double-pomeron gluon cross sections to the parity even/odd double-pomeron isosinglet cross sections by multiplying the formers with $(\sqrt{2N_f} \sigma_*^2 \rho^4)^2$ (even) and $(\sqrt{2N_f} \chi_* \rho^4)^2$ (odd). The η_0 is a mixture of η', η with mixing angle $\theta_M \approx 20^\circ$.

Putting everything together, it follows that the double-pomeron production of η' in pp scattering is given respectively by

$$\frac{1}{N_c^2} \frac{d\sigma_{\eta'}}{dq_{1\perp} dq_{2\perp} d\eta} = \left(\sqrt{2N_f} \chi_* \rho^4 \cos(\theta_M) \right)^2 \sin^2 \phi \times \mathbf{C}_S \pi \rho^2 |\mathbf{J}(q_{1\perp})|^2 |\mathbf{J}(q_{2\perp})|^2 \sigma_S(m_{\eta'}^2) \quad (40)$$

while the double-pomeron production of heavy isosinglet scalars reads

$$\frac{1}{N_c^2} \frac{d\sigma_s}{dq_{1\perp} dq_{2\perp} d\eta} = \left(\sqrt{2N_f} \sigma_*^2 \rho^4 \right)^2 \cos^2 \phi \times \mathbf{C}_S \pi \rho^2 |\mathbf{J}(q_{1\perp})|^2 |\mathbf{J}(q_{2\perp})|^2 \sigma_S(m_s^2). \quad (41)$$

VII. EXCLUSIVE DOUBLE-POMERON: WA102

The most natural general prediction which follows from our approach is that since the inclusive clusters are predicted to have a mass of about 3 GeV, the exclusive

glueball states – such as the scalar at 1.7 GeV and pseudoscalar above 2 GeV – can be significant. As the latter has not yet been identified experimentally, we focused instead on the η' , known to interact strongly with the glue.

The ϕ dependence is the most dazzling empirical feature of WA102. The data exhibit different azimuthal dependence of the partial cross section for various J^{PC} quantum numbers of the final states. In Fig. 3 we show the dependence on ϕ for two 0^{-+} channels, η, η' , which is clearly $\sin^2(\phi)$. This is in complete agreement with the dependence expected from our calculations. On the other hand for the scalar glueball the WA102 finds a distribution with a maximum at $\phi = 0$ (not shown here). In this case, we predict $\cos^2(\phi)$.

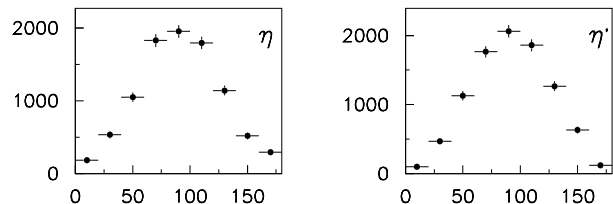


FIG. 3. Dependence of the double-pomeron cross section on the azimuthal angle ϕ for 0^{-+} production in the final states from Ref. [18]

The **t -dependence** is also very important to compare. As shown in our previous paper [2], the form-factor basically represents the size and the shape of the instantons, and although the latter is established rather well with $\rho \approx 0.3$ fm [1], the shape is not. So identifying the observed t dependence with our formfactor one can learn about the actual shape of the instantons in the QCD vacuum.

The measured dependence on the transverse momentum $|t|$ is shown in Fig. 4. It is best parametrized as [18] $\beta |t|^n e^{-b|t|}$ with $n \approx 1 - 2$, $10^3 \beta \approx 110$ and $b \approx 11$ GeV $^{-2}$. This dependence in our case is carried by the \mathbf{F}^4 factor in the differential cross section. The dependence of \mathbf{F} on $\sqrt{-t}$ in units of the instanton size is shown in Fig. 5 for $\mathbf{a} = 0, 1/4, 1/2, 3/4$. Clearly, the empirical results are in agreement with a non-vanishing \mathbf{a} as originally suggested in [2], and in disagreement with the Pomeron expectation. For large $|t|$ the sphaleron induced form factor falls as $e^{-6\rho\sqrt{-t}}$ with $6\rho \approx 7$ GeV $^{-1}$.

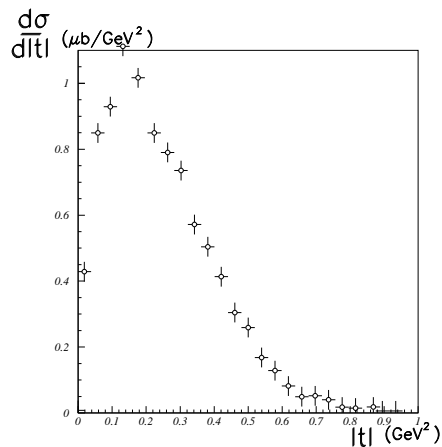


FIG. 4. The WA102 measured dependence of the double-pomeron cross section for η' production on the momentum transfer $|t|$ [19].

The next Fig.5 compares this experimental t -dependence from $(d\sigma/dt)^{1/4}$ to the instanton formfactor. The 4 theoretical curves are from our previous paper [2]. They show the predicted shape for 4 values of the instanton tail modification parameter a . The experimental points show the same shape as predicted. Furthermore, they are right in the middle of the a interval assumed, so that $a \approx 1/3$ would fit very well. Note that the relative errors (which are not shown) are large for points on the right side of the experimental quotes.

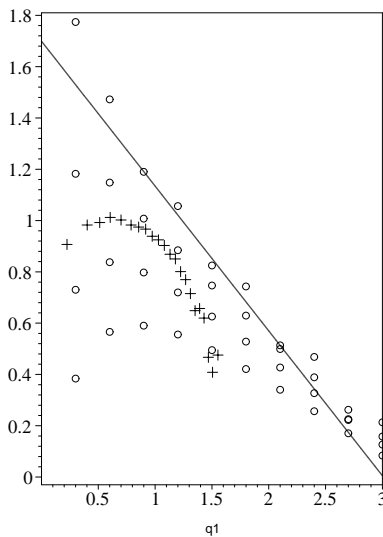


FIG. 5. The log of the form factor $|\mathbf{J}(q_{\perp})|$ versus $q1 = \rho\sqrt{-t}$ where ρ is the instanton size. The 4 theoretical curves are for the instanton shape parameter $\mathbf{a} = 0, 1/4, 1/2, 3/4$ (top to bottom) [2]. The crosses show the data points (without error bars) of the data shown in the previous figure, as $(d\sigma/dt)^{1/4}$ with the same units of $q1$ (arbitrary normalization).

An estimate of the η' cross section in pp double-pomeron follows from our projected result (40), i.e.

$$\frac{\sigma(\eta')}{\sigma_{IN}} \approx (0.125) \times (6 \cdot 10^{-4}) \times (10^{-1}) . \quad (42)$$

where the first factor is due to the singlet projection, the second factor to the η' projection and the third factor to the fact that the η' mass is lower than the sphaleron mass which is an extra penalty in the partial cross section. For $\sigma_{IN} \approx 30$ mb at $\sqrt{s} \approx 30$ GeV, we predict $\sigma(\eta') \approx 225$ nb in comparison to the 588 nb observed empirically [18].

VIII. CONCLUSIONS

We have addressed the issue of inclusive and exclusive double-pomeron scattering in the semi-hard regime, using the semiclassical theory of high energy collisions recently developed. We have found that it works remarkably well, explaining even such details as correlation between the azimuthal distributions and quantum numbers of the cluster.

We have shown that the semiclassical double-pomeron cross section relates simply to the semiclassical inelastic cross section: overall it is about 10% of the latter due to an extra gluon and extra color restrictions. This corresponds to a large cross section in absolute magnitude, well above the Pomeron factorization, as the UA8 experiment indeed observed. We also have shown that all the distributions of the UA8 inclusive data over 6-d kinematical space is quite compatible with our predictions.

The exclusive results from WA102 experiment seem to confirm this theory even more. We have a very good agreement for scalar glueball and η' productions, which show very different azimuthal dependence.

As example of a disagreement let us mention that in our theory central double-pomeron semiclassical production of η is found to be suppressed by almost 2 orders of magnitude in comparison to η' : a suppression of 10^{-1} is due to the mixing angle, and an extra suppression of 10^{-1} is due to its lower mass in the partial cross section. This strong suppression is not observed. We think that all light hadrons such as η and π^0 and possibly $f_0(600)$ are too far from the sphaleron mass scale of about 3 GeV to be reliably calculated in the same manner. We currently suspect their production to rely on a different mechanism, and will report on it elsewhere.

Since some sense has been made of the single- and double-pomeron physics in the context of semiclassical dynamics of the gauge fields, related with tunneling and topoly, new rounds of experiments seem to be justified in this context more than ever. We believe that the RHIC detectors and especially STAR can do a lot in the pp mode, with and without diffraction. Clearly they have a potential to clarify further the nature and characteristics of the central production in the semi-hard regime.

Acknowledgments

This work was supported in parts by the US-DOE grant DE-FG-88ER40388. One of us I.Z. would like to thank V. Vento for discussions and La Comisión de Intercambio Cultural, Educativo y Científico entre España y Estados Unidos de América for supporting his visit to the University of Valencia where this work was initiated. We both thank P.Schlein for his comments on the manuscript and G. Papp for help with some of the figures.

- [1] T. Schafer and E. V. Shuryak, *Rev. Mod. Phys.* **70** (1998) 323.
- [2] E. Shuryak and I. Zahed, *Phys. Rev.* **D62** (2000) 085014; M. Nowak, E. Shuryak and I. Zahed, *Phys. Rev.* **D64** (2001) 034008.
- [3] D. Kharzeev, Y. Kovchegov and E. Levin, *Nucl. Phys.* **A690** (2001) 621.
- [4] F. Schrempp and A. Utermann, [hep-ph/0207052](#).
- [5] D. M. Ostrovsky, G. W. Carter and E. V. Shuryak, *Phys. Rev.* **D66** (2002) 036004.
- [6] R. Janik, E. Shuryak and I. Zahed, [hep-ph/0206005](#).
- [7] E. Shuryak and I. Zahed, [hep-ph/0206022](#)
- [8] A. Giovannini and R. Ugoccioni, [hep-ph/0209040](#).
- [9] UA8 Collaboration (A. Brandt et al.), *Eur.Phys.J.C* **25** (2002) 361, [hep-ex/0205037](#).
- [10] F. Close and A. Kirk, *Phys. Lett.* **B397** (1997) 333; F. Close, *Phys. Lett.* **B419** (1998) 387.
- [11] J. Ellis and D. Kharzeev, [hep-ph/9811222](#).
- [12] N. Kochelev, [hep-ph/9902203](#)
- [13] F. Low, *Phys. Rev.* **D12** (1975) 163; S. Nussinov, *Phys. Lett.* **34** (1975) 1286.
- [14] D. Diakonov and V. Petrov, *Phys. Rev.* **D 50** (1994) 266.
- [15] A. Donnachie and P. Landshoff, *Nucl. Phys.* **B303** (1988) 634.
- [16] G. W. Carter, D. M. Ostrovsky and E. V. Shuryak, *Phys. Rev.* **D65** (2002) 074034
- [17] M. Kacir, M. Prakash and I. Zahed, *Act. Phys. Pol.* **B30** (1999) 287; [hep-ph/9602314](#).
- [18] A. Kirk, [hep-ph/9810221](#).
- [19] N. Kochelev, T. Morii and A. Vinnikov, [hep-ph/9903279](#).